PHYSICAL REVIEW D **90,** 071301(R) (2014)

Status of Higgs couplings after run 1 of the LHC

Jérémy Bernon,[*] Béranger Dumont,[†] and Sabine Kraml[‡]

Laboratoire de Physique Subatomique et de Cosmologie (LPSC), Université Grenoble-Alpes, CNRS/IN2P3, 53 Avenue des Martyrs, F-38026 Grenoble, France

(Received 10 September 2014; published 17 October 2014)

We provide an update of the global fits of the couplings of the 125.5 GeV Higgs boson using all publicly available experimental results from run 1 of the LHC as per summer 2014. The fits are done by means of the new public code LILITH 1.0. We present a selection of results given in terms of signal strengths, reduced couplings, and for the two-Higgs-doublet models of type I and II.

DOI: 10.1103/PhysRevD.90.071301 PACS numbers: 14.80.Bn, 14.80.Ec

I. INTRODUCTION

The properties of the observed Higgs boson with mass around 125 GeV [1,2] have been measured with unforeseeable precision already during run 1 of the LHC at 7–8 TeV center-of-mass energy [3,4]. This is a consequence of the excellent operation of the LHC and of the wealth of accessible final states for a 125 GeV Standard Model (SM)-like Higgs boson. Indeed, many distinct signal strengths, defined as production × decay rates relative to SM expectations, $\mu_i \equiv (\sigma \times \mathcal{B})_i/(\sigma \times \mathcal{B})_i^{\rm SM}$, have been measured and used to obtain information about the couplings of the Higgs boson to electroweak gauge bosons, fermions of the third generation, and loop-induced couplings to photons and gluons. (See [5] for a thorough discussion of the use of signal strengths μ_i.)

Fits to various combinations of reduced Higgs couplings, i.e., Higgs couplings to fermions and gauge bosons relative to their SM values, have been performed by the experimental collaborations themselves, e.g., in [3,4]. Moreover, theorists combine the results from ATLAS and CMS in global fits (see, e.g., [6,7] and references therein) in order to test consistency with SM expectations and to constrain models with modified Higgs couplings. In particular, the couplings of the observed Higgs boson could deviate from the SM predictions due to the presence of other Higgs states mixing with the observed one and/or due to new particles contributing to the loop-induced couplings.

In [6], a comprehensive analysis of the Higgs signal strengths and couplings and implications for extended Higgs sectors was performed based on the experimental results as per Spring 2013. Since then, a number of new measurements or updates of existing ones were published by the experimental collaborations. From ATLAS, the VH, $H \to b\bar{b}$ and the $H \to \tau\tau$ results were updated with full luminosity [8,9]. Moreover, significantly improved measurements in the $H \to \gamma\gamma$ [10] and $H \to ZZ^*$ [11] channels were released, and the search for invisible decays in the $ZH \to \ell\ell +$ invisible channel was updated [12]. There were also significant news from CMS, in particular updates of the $H \to ZZ^* \to 4\ell$ [13] and $H \to WW^*$ [14] results, and—most importantly—the long-awaited final results for the $H \to \gamma\gamma$ channels [15]. Furthermore, CMS published new results for $H \to \tau\tau$ [16] and $H \to$ invisible [17]. Finally, in both ATLAS and CMS a special effort was made for probing the production of a Higgs boson in association with a pair of top quarks (ttH). From ATLAS, ttH results are available for $H \to \gamma\gamma$ [10] and $H \to b\bar{b}$ [18], while CMS published ttH results for $H \to \gamma\gamma$, $b\bar{b}$, $\tau\tau$, ZZ^* and WW^* [19].

We therefore think that an update of the global coupling fits, combining ATLAS and CMS results, is timely and interesting for the high-energy-physics community in general, even more so as this will likely define the status of the Higgs couplings until the first round of Higgs results will become available from LHC Run-2 (or until an official combination of the run 1 results is done by ATLAS and CMS). Hence, in this short communication, we provide such an update for (i) the combined signal strengths, (ii) the most important reduced coupling fits, and (iii) two Higgs doublet models of type I and type II by means of a new public code, LILITH 1.0 [20].

LILITH stands for "LIght LIkelihood fiT for the Higgs." It is a light and easy-to-use PYTHON tool to determine the likelihood of a generic Higgs boson with mass around 125 GeV from the latest experimental data, and can conveniently be used to fit the Higgs couplings and/or put constraints on theories beyond the SM. The experimental results used are the signal strengths in the primary Higgs production modes [21] as published by the ATLAS and CMS experiments at the LHC and by the Tevatron experiments. All experimental data are stored in a flexible XML database which is easy to maintain. LILITH 1.0 has been validated extensively against the ATLAS and CMS coupling fits, see [20]. A quick user guide is also available from [20]; a manual providing a complete description of the code is in preparation.

[*]jeremy.bernon@lpsc.in2p3.fr
[†]beranger.dumont@lpsc.in2p3.fr
[‡]sabine.kraml@lpsc.in2p3.fr

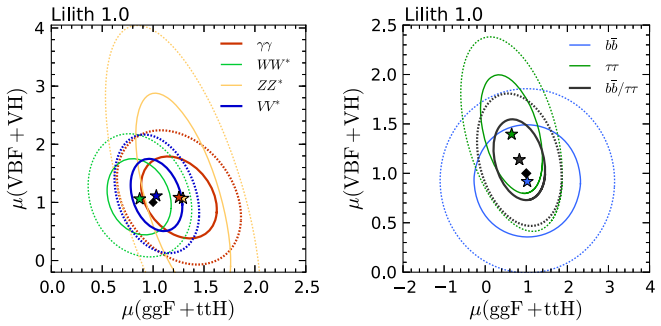

FIG. 1 (color online). Combined signal strengths in the plane of (ggF + ttH) versus (VBF + VH) production, on the left for the $\gamma\gamma$, ZZ^*, WW^* and VV^* decay modes (the latter assuming $ZZ^* = WW^*$), on the right for the $b\bar{b}$ and $\tau\tau$ decay modes and their combination $b\bar{b} = \tau\tau$. The full (dashed) contours denote the 68.3% (95.4%) C.L. regions, derived by combining the ATLAS, CMS, and Tevatron results. The best-fit points are marked as stars, and the SM case by a black diamond.

II. COMBINED SIGNAL STRENGTHS

We begin by showing in Fig. 1 contours of constant confidence level (C.L.) for the combined signal strengths in the $\mu(\text{ggF} + \text{ttH})$ versus $\mu(\text{VBF} + \text{VH})$ plane for different Higgs decay modes. The left panel shows the bosonic channels $H \to \gamma\gamma$, WW^*, ZZ^* as well as VV^*, where $VV^* \equiv ZZ^*$, WW^*; the right panel shows the fermonic channels $b\bar{b}$, $\tau\tau$ as well as $b\bar{b} = \tau\tau$.

The combination of the ZZ^* and WW^* decay modes is justified by custodial symmetry, which implies that the HZZ and HWW couplings are rescaled by the same factor with respect to the SM. The combination of the $b\bar{b}$ and $\tau\tau$ decay modes is justified, in principle, in models where one specific Higgs doublet has the same couplings, with respect to the SM, to down-type quarks and leptons, although QCD corrections can lead to deviations of the reduced Hbb and $H\tau\tau$ couplings from a common value.

All results show an excellent agreement with the SM. Compared to [6], uncertainties have been significantly reduced for the fermionic channels, particularly for $H \to b\bar{b}$ in ttH production. As for $H \to \gamma\gamma$, while previously small excesses were observed in ggF by ATLAS and in VBF + VH by both ATLAS and (to a lesser extent) CMS, updated results point to a more SM-like behavior. At the same time, the slight deficit previously seen by CMS in ggF is no longer present. Overall, this leads to a central value only slightly larger than unity.

A comment is in order here. In the latest experimental papers, only the 68% and 95% C.L. contours are displayed in the $\mu(\text{ggF} + \text{ttH})$ versus $\mu(\text{VBF} + \text{VH})$ plots, or in other two-dimensional projections. In order to use this information, one is forced to make assumptions on the likelihood functions—typically this means assuming normally distributed signal strengths, and this is also the approach we have adopted here. However, this is not fully satisfactory and sometimes reproduces the contours rather poorly, as in the case of ATLAS $H \to ZZ^*$. (See [5] for a detailed discussion.) In the previous round of Higgs results, CMS had provided a temperature plot for the $H \to \gamma\gamma$ result [15], while ATLAS had gone a step further and digitally published the two-dimensional likelihood grids for the bosonic channels [22–24] corresponding to the results of [25]. This was a boon for interpretation studies, as it rendered the Gaussian approximation unnecessary at least for these channels. We strongly hope that such likelihood grids (or digitized temperature plots) will again be made available in the future by both ATLAS and CMS.

In the Gaussian approximation, we can derive a simple expression for the χ^2 for each decay mode j in the form of ellipses [6]

$$\chi_j^2 = a_j(\mu_j^{\text{ggF}} - \hat{\mu}_j^{\text{ggF}})^2 + c_j(\mu_j^{\text{VBF}} - \hat{\mu}_j^{\text{VBF}})^2 + 2b_j(\mu_j^{\text{ggF}} - \hat{\mu}_j^{\text{ggF}})(\mu_j^{\text{VBF}} - \hat{\mu}_j^{\text{VBF}}), \quad (1)$$

where the upper indices ggF and VBF stand for (ggF + ttH) and (VBF + VH), respectively, and $\hat{\mu}_j^{\text{ggF}}$ and $\hat{\mu}_j^{\text{VBF}}$ denote the best-fit points obtained from the measurements. The parameters $\hat{\mu}^{\text{ggF}}$, $\hat{\mu}^{\text{VBF}}$, a, b, and c for Eq. (1) (and, for completeness, the correlation coefficient ρ) resulting from our fit are listed in Table I. Approximating the χ^2 in this form can be useful for applications that aim at a quick assessment of the compatibility with the experimental data without invoking the complete likelihood calculation. In the fits presented below, we will apply the full machinery of LILITH 1.0.

TABLE I. Combined best-fit signal strengths $\hat{\mu}^{\text{ggF}}$, $\hat{\mu}^{\text{VBF}}$ and correlation coefficient ρ for various Higgs decay modes (with $VV^* \equiv WW^*$, ZZ^*), as well as the coefficients a, b and c for the approximate χ^2 in Eq. (1).

	$\hat{\mu}^{\text{ggF}}$	$\hat{\mu}^{\text{VBF}}$	ρ	a	b	c
$\gamma\gamma$	1.25 ± 0.24	1.09 ± 0.46	−0.30	18.26	2.84	5.08
VV^*	1.03 ± 0.17	1.12 ± 0.41	−0.29	39.07	4.68	6.52
ZZ^*	1.30 ± 0.31	1.06 ± 1.20	−0.59	16.27	2.45	1.06
WW^*	0.86 ± 0.21	1.09 ± 0.43	−0.20	24.15	2.29	5.58
$b\bar{b}/\tau\tau$	0.83 ± 0.41	1.14 ± 0.27	−0.27	6.29	2.62	14.86
$b\bar{b}$	1.02 ± 0.85	0.92 ± 0.38	0	1.37	0	7.10
$\tau\tau$	0.64 ± 0.50	1.40 ± 0.40	−0.42	4.92	2.60	7.76

III. FITS TO REDUCED HIGGS COUPLINGS

Let us now turn to the fits of reduced couplings. To this end, we define

$$\mathcal{L} = \left[C_W m_W W^\mu W_\mu + C_Z \frac{m_Z}{\cos\theta_W} Z^\mu Z_\mu - C_U \frac{m_t}{2m_W} \bar{t}t - C_D \frac{m_b}{2m_W} \bar{b}b - C_D \frac{m_\tau}{2m_W} \bar{\tau}\tau \right] H, \quad (2)$$

where the C_I are scaling factors for the couplings relative to their SM values, introduced to test possible deviations in the data from SM expectations. We set C_W, $C_Z > 0$ by convention; custodial symmetry implies $C_V \equiv C_W = C_Z$.

In addition to these tree-level couplings, we define the loop-induced couplings C_g and C_γ of the H to gg and $\gamma\gamma$, respectively. With the BEST-QCD option in LILITH 1.0, the contributions of SM particles to C_g and C_γ (as well as the corrections to VBF production) are computed at NLO QCD from the given values for C_U, C_D, C_W, and C_Z following the procedure recommended by the LHC Higgs Cross Section Working Group [26] (using grids generated from HIGLU [27], HDECAY [28], and VBFNLO [29]). Alternatively, C_g and C_γ can be taken as free parameters. Finally, invisible or undetected branching ratios can also be included in the fit.

Deviations from SM expectations can be divided into two categories: (i) modifications of the tree-level couplings, as in extended Higgs sectors or Higgs portal models, and (ii) vertex loop effects from new particles beyond the SM, modifying in particular C_g and/or C_γ. We first discuss the former.

Figure 2 shows results for a three-parameter fit of C_U, C_D, C_V, assuming custodial symmetry and taking C_U, $C_D > 0$. We note that at 95.4% C.L. in two dimensions, C_U and C_V are constrained within roughly $\pm 20\%$; the uncertainty on C_D is about twice as large. Although not shown in Fig. 2, $C_U < 0$ is excluded at more than 2σ, while the sign ambiguity in C_D remains. (See [30] for a discussion of wrong-sign Yukawa couplings.) The fact that $\hat{\mu}_{\gamma\gamma}^{\mathrm{ggF}}$, $\hat{\mu}_{\gamma\gamma}^{\mathrm{VBF}}$, and $\hat{\mu}_{VV}^{\mathrm{VBF}}$ lie somewhat above one (cf. Fig. 1 and Table I) leads to a slight preference for $C_V > 1$. The best fit is obtained for $C_U = C_D = 1.01$ and $C_V = 1.05$, resulting in $C_g = 1.01$ and $C_\gamma = 1.06$. All these reduced couplings are however consistent with unity at the 1σ level. In one dimension, i.e., profiling over the other parameters, we find $C_U = [0.91, 1.11]$ ([0.82,1.22]), $C_D = [0.85, 1.16]$ ([0.70,1.32]), and $C_V = [0.97, 1.13]$ ([0.89,1.20]) at 68.3% (95.4%) C.L.; requiring $C_V < 1$, we get $C_V > 0.96$ (0.88).

To test possible deviations from custodial symmetry, we next define $C_{WZ} \equiv C_W/C_Z$ and perform a four-parameter fit of C_U, C_D, C_Z, C_{WZ}. In one dimension, we find $C_{WZ} = [0.83, 1.02]$ ([0.75,1.16]) and $C_Z = [1.0, 1.24]$ ([0.89,1.35]) at 68.3% (95.4%) C.L. (The corresponding 68.3% and 95.4% C.L. intervals for C_W are [0.95,1.11] and [0.87, 1.19].) Current Higgs data hence provide a significant constraint on deviations from custodial symmetry.

So far, we considered deviations of the tree-level reduced couplings from unity, but no extra loop contributions to the effective couplings to gluons and/or photons. If instead we fix $C_{U,D,V}$ but allow C_g and C_γ to vary freely, corresponding to loop contributions ΔC_g, ΔC_γ from new physics, we obtain the result shown in Fig. 3. (In this case, $C_{g,\gamma} = \bar{C}_{g,\gamma} + \Delta C_{g,\gamma}$, with $\bar{C}_{g,\gamma}$ the contribution from SM particles.) The left panel corresponds to the case where $C_U = C_D = C_V = 1$; here the best-fit point has $\Delta C_g = -0.01$ and $\Delta C_\gamma = 0.09$, as expected from Fig. 1. The right panel shows the situation when C_U, C_D, C_V are fixed to the best-fit values previously obtained: $C_U = C_D = 1.01$, $C_V = 1.05$; in this case the best-fit point has $\Delta C_g = -0.04$ and $\Delta C_\gamma = 0.06$. In both cases, the SM solution $\Delta C_g = \Delta C_\gamma = 0$ lies within the 1σ contour.

The current status of invisible (unseen) decays is as follows (all limits at 95.4% C.L.):

(i) for SM-like couplings, $\mathcal{B}_{\mathrm{inv}} < 0.12$ ($\mathcal{B}_{\mathrm{new}} < 0.09$),

(ii) for $C_{U,D,V} = 1$ but C_g, C_γ free, we find $\mathcal{B}_{\mathrm{inv}} < 0.24$ ($\mathcal{B}_{\mathrm{new}} < 0.23$),

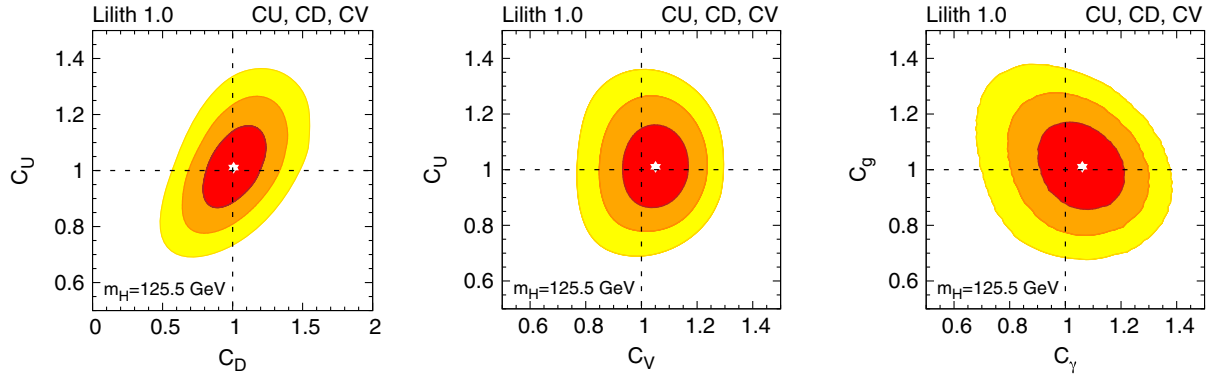

FIG. 2 (color online). Fits of C_U, C_D, and C_V (left and middle panels) and resulting C_g versus C_γ (right panel). The central (red), intermediate (orange) and outer (yellow) areas are the 68.3%, 95.4%, and 99.7% C.L. regions, respectively. The best-fit points are marked as white stars. Invisible or undetected decays are assumed to be absent.

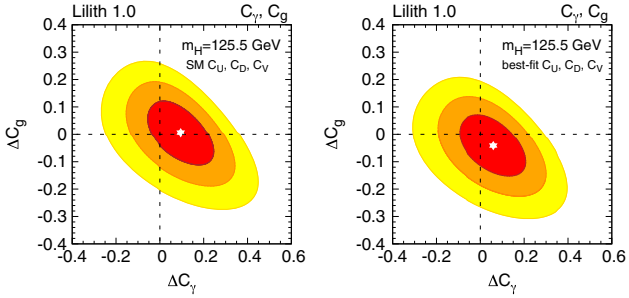

FIG. 3 (color online). As Fig. 2 but for a two-parameter fit of C_g and C_γ; in the left panel $\Delta C_g = C_g - 1$, $\Delta C_\gamma = C_\gamma - 1$ (SM values of C_U, C_D, C_V), while in the right panel C_U, C_D, C_V are fixed to their best-fit values and hence $\Delta C_g = C_g - 1.01$, $\Delta C_\gamma = C_\gamma - 1.06$.

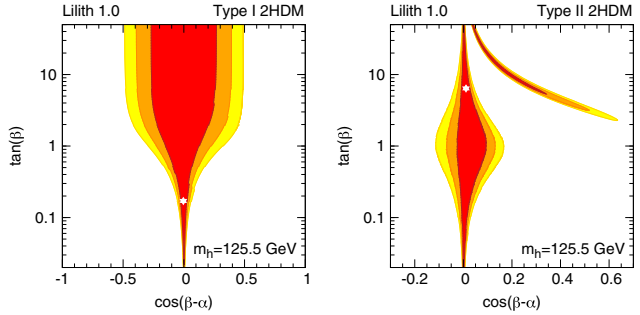

FIG. 4 (color online). Fits of $\cos(\beta-\alpha)$ versus $\tan\beta$ for the 2HDM of type I (left) and of type II (right) for $m_h = 125.5$ GeV. The central (red), intermediate (orange) and outer (yellow) areas are the 68.3%, 95.4%, and 99.7% C.L. regions, respectively. The best-fit points are marked as white stars. Decays into non-SM particles (such as $h \to AA$) are assumed to be absent.

(iii) for free C_U, C_D, C_V but $C_V < 1$, we find $\mathcal{B}_{\rm inv} < 0.24$ ($\mathcal{B}_{\rm new} < 0.22$); this increases to $\mathcal{B}_{\rm inv} < 0.34$ when C_V is unconstrained (in this case no limit on $\mathcal{B}_{\rm new}$ can be obtained [6]).

IV. TWO-HIGGS-DOUBLET MODELS

In view of the discussion above it is clear that models with an extended Higgs sector will be significantly constrained by the data. In particular, it is interesting to consider the simplest such extensions of the SM, namely two-Higgs-doublet models (2HDMs) of type I and type II. The basic parameters describing the couplings of the neutral Higgs states to SM particles are only two: the CP-even Higgs mixing angle α and the ratio of the vacuum expectation values, $\tan\beta = v_u/v_d$. The couplings, normalized to their SM values, of the Higgs bosons to vector bosons (C_V) and to up- and down-type fermions (C_U and C_D) are functions of α and β as given in Table II; see, e.g., [31] for details. The type I and type II models are distinguished only by the pattern of their fermionic couplings.

To investigate the impact of the current Higgs data on 2HDMs, we vary $\alpha = [-\pi/2, +\pi/2]$ and $\beta = [0, \pi/2[$. (Note that this results in $C_U > 0$ in our convention, while C_V can be negative). We implicitly assume that there are no contributions from non-SM particles to the loop diagrams for C_γ and C_g. In particular, this means our results correspond to the case where the charged Higgs boson, whose loop might contribute to C_γ, is heavy.

TABLE II. Tree-level couplings C_V, C_U, C_D for the two scalars h, H and the pseudoscalar A in type I and type II 2HDMs; $s_\alpha \equiv \sin\alpha$, $c_\alpha \equiv \cos\alpha$, $s_\beta \equiv \sin\beta$, $c_\beta \equiv \cos\beta$.

	Type I and II	Type I		Type II	
Higgs	C_V	C_U	C_D	C_U	C_D
h	$\sin(\beta-\alpha)$	c_α/s_β	c_α/s_β	c_α/s_β	$-s_\alpha/c_\beta$
H	$\cos(\beta-\alpha)$	s_α/s_β	s_α/s_β	s_α/s_β	c_α/c_β
A	0	$\cot\beta$	$-\cot\beta$	$\cot\beta$	$\tan\beta$

The results of the 2HDM fits are shown in Fig. 4 for the case that the observed state at 125.5 GeV is the lighter CP-even h. In the case of the type I model, we note a broad valley along the SM limit of $\cos(\beta-\alpha) = 0$, which is rather flat in $\tan\beta$. For $\tan\beta \gtrsim 2$, at 95.4% C.L. $|\cos(\beta-\alpha)|$ can be as large as $\approx$0.4; only for $\tan\beta \ll 1$, one is forced into the decoupling/alignment regime. The situation is quite different for the type II model. Here we observe two narrow valleys in the $\tan\beta$ versus $\cos(\beta-\alpha)$ plane. The first one lies along the SM solution $\cos(\beta-\alpha) = 0$; the largest deviation here occurs around $\tan\beta \approx 1$, where $\cos(\beta-\alpha) \approx 0.13$ is allowed at 95.4% C.L.; for both $\tan\beta \gg 1$ and $\tan\beta \ll 1$ one is forced into the decoupling/alignment regime. The second minimum is a banana-shaped valley with $\tan\beta \gtrsim 3$ (5) and $\cos(\beta-\alpha) \lesssim 0.35$ (0.5) at 68.3% (95.4%) C.L. This corresponds to the degenerate solution with $C_D \approx -1$. In one dimension, the 68.3% (95.4%) C.L. limits are $|\cos(\beta-\alpha)| < 0.19$ (0.34) for type I and $\cos(\beta-\alpha) = [0, 0.29]$ ($[-0.05, 0.47]$) for type II; the latter shrinks to $\cos(\beta-\alpha) = [0, 0.07]$ ($[-0.05, 0.11]$) when demanding $C_D > 0$.

Constraints on and future prospects for 2HDMs in light of the LHC Higgs signal (status spring 2013) were discussed in detail in [32] taking into account all relevant theoretical and experimental constraints. The results of that paper will be somewhat modified by the new constraints presented here; this is presently under study.

V. CONCLUSIONS

We presented a brief update of the global fits of the 125.5 GeV Higgs boson using all publicly available experimental results as per summer 2014. The fits were done with LILITH 1.0, a new user-friendly public tool for evaluating the likelihood of an SM-like Higgs boson in view of the experimental data. Our results can be summarized as follows:

(1) The latest ATLAS and CMS results for the $H \to \gamma\gamma$ decay mode now point to a very good agreement with the SM; concretely we get $\hat{\mu}_{\gamma\gamma}^{\mathrm{ggF+ttH}} = 1.25 \pm 0.24$ and $\hat{\mu}_{\gamma\gamma}^{\mathrm{VBF+VH}} = 1.09 \pm 0.46$ with a correlation of $\rho = -0.30$.
(2) In the C_U, C_D, C_V reduced coupling fit, we found $C_U = 1.01 \pm 0.1$, $C_D = 1.01 \pm 0.16$ and $C_V = 1.05 \pm 0.08$; in terms of the loop-induced couplings this corresponds to $C_g = 1.01 \pm 0.11$ and $C_\gamma = 1.06 \pm 0.11$ (in one dimension).
(3) Custodial symmetry can also be tested. We found $C_{WZ} = 0.92 \pm 0.1$, hence compatibility with custodial symmetry at the 1σ level.
(4) Assuming SM-like couplings, the limit for invisible decays is $\mathcal{B}_{\mathrm{inv}} < 0.12$ at 95.4% C.L. This changes to $\mathcal{B}_{\mathrm{inv}} < 0.34$ when C_U, C_D, C_V (or even C_U, C_D, C_V, C_g, C_γ) are allowed to vary.
(5) In the context of 2HDMs, barring loop contributions from the charged Higgs, the 95.4% C.L. limits in one dimension are $\sin(\beta - \alpha) > 0.94$ in type I and $\sin(\beta - \alpha) > 0.90$ in type II.

As mentioned, one of the limitations of these fits is the use of the Gaussian approximation. This could easily be avoided if the experimental collaborations published the two-dimensional likelihood grids in addition to the 68% and 95% C.L. contours. Another limitation is induced by the combination of production modes, typically ggF + ttH and VBF + VH, in the experimental results. This could be overcome if the collaborations provided the signal strength likelihoods beyond two-dimensional projections—the optimum would be to have the signal strengths as functions of m_H separated into all five production modes ggF, ttH, VBF, ZH, and WH, as recommended in [5]. We hope that this way of presentation (in digital form) will be adopted for Higgs results at run 2 of the LHC. The structure of LILITH is well suited to make use of such extended experimental results.

ACKNOWLEDGMENTS

We thank John F. Gunion and Yun Jiang for discussions. J. B. is supported by the "Investissements d'avenir, Labex ENIGMASS."

[1] ATLAS Collaboration, Phys. Lett. B **716**, 1 (2012).
[2] CMS Collaboration, Phys. Lett. B **716**, 30 (2012).
[3] ATLAS Collaboration, Report No. ATLAS-CONF-2014-009.
[4] CMS Collaboration, Report No. CMS-PAS-HIG-14-009.
[5] F. Boudjema *et al.*, arXiv:1307.5865.
[6] G. Belanger, B. Dumont, U. Ellwanger, J. Gunion, and S. Kraml, Phys. Rev. D **88**, 075008 (2013).
[7] B. Dumont, J. F. Gunion, and S. Kraml, Phys. Rev. D **89**, 055018 (2014).
[8] ATLAS Collaboration, Report No. ATLAS-CONF-2013-079.
[9] ATLAS Collaboration, Report No. ATLAS-CONF-2013-108.
[10] ATLAS Collaboration, arXiv:1408.7084.
[11] ATLAS Collaboration, arXiv:1408.5191.
[12] ATLAS Collaboration, Phys. Rev. Lett. **112**, 201802 (2014).
[13] CMS Collaboration, Phys. Rev. D **89**, 092007 (2014).
[14] CMS Collaboration, J. High Energy Phys. 01 (2014) 096.
[15] CMS Collaboration, arXiv:1407.0558.
[16] CMS Collaboration, J. High Energy Phys. 05 (2014) 104.
[17] CMS Collaboration, Eur. Phys. J. C **74**, 2980 (2014).
[18] ATLAS Collaboration, Report No. ATLAS-CONF-2014-011.
[19] CMS Collaboration, J. High Energy Phys. 09 (2014) 087.
[20] J. Bernon and B. Dumont, http://lpsc.in2p3.fr/projects-th/lilith/.
[21] The five theoretically "pure" production modes that are accessible are gluon-gluon fusion (ggF), vector-boson fusion (VBF), associated production with a W or Z boson (WH and ZH, commonly denoted as VH), and associated production with a top-quark pair (ttH).
[22] ATLAS Collaboration, http://doi.org/10.7484/INSPIREHEP.DATA.A78C.HK44.
[23] ATLAS Collaboration, http://doi.org/10.7484/INSPIREHEP.DATA.RF5P.6M3K.
[24] ATLAS Collaboration, http://doi.org/10.7484/INSPIREHEP.DATA.26B4.TY5F.
[25] ATLAS Collaboration, Phys. Lett. B **726**, 88 (2013).
[26] A. David *et al.* (LHC Higgs Cross Section Working Group), arXiv:1209.0040.
[27] M. Spira, arXiv:hep-ph/9510347.
[28] A. Djouadi, J. Kalinowski, and M. Spira, Comput. Phys. Commun. **108**, 56 (1998).
[29] K. Arnold, J. Bellm, G. Bozzi, M. Brieg, F. Campanario *et al.*, arXiv:1107.4038.
[30] P. Ferreira, J. F. Gunion, H. E. Haber, and R. Santos, Phys. Rev. D **89**, 115003 (2014).
[31] J. F. Gunion, H. E. Haber, G. L. Kane, and S. Dawson, Front. Phys. **80**, 1 (2000).
[32] B. Dumont, J. F. Gunion, Y. Jiang, and S. Kraml, Phys. Rev. D **90**, 035021 (2014).